The Journal of Chemical Physics

Rotational and translational self-diffusion in concentrated suspensions of permeable particles

Gustavo C. Abade, Bogdan Cichocki, Maria L. Ekiel-Jeżewska, Gerhard Nägele, and Eligiusz Wajnryb

Citation: J. Chem. Phys. **134**, 244903 (2011); doi: 10.1063/1.3604813
View online: http://dx.doi.org/10.1063/1.3604813
View Table of Contents: http://jcp.aip.org/resource/1/JCPSA6/v134/i24
Published by the American Institute of Physics.

Rotational and translational self-diffusion in concentrated suspensions of permeable particles

Gustavo C. Abade,[1] Bogdan Cichocki,[2] Maria L. Ekiel-Jeżewska,[3,a)] Gerhard Nägele,[4] and Eligiusz Wajnryb[3]

[1]*Departamento de Engenharia Mecânica, Faculdade de Tecnologia, Universidade de Brasília, Campus Universitário Darcy Ribeiro, 70910-900 Brasília-DF, Brazil*
[2]*Institute of Theoretical Physics, Faculty of Physics, University of Warsaw, Hoża 69, 00-681 Warsaw, Poland*
[3]*Institute of Fundamental Technological Research, Polish Academy of Sciences, Pawińskiego 5B, 02-106 Warsaw, Poland*
[4]*Institute of Complex Systems (ICS-3), Research Centre Jülich, D-52425 Jülich, Germany*

(Received 19 March 2011; accepted 6 June 2011; published online 29 June 2011)

In our recent work on concentrated suspensions of uniformly porous colloidal spheres with excluded volume interactions, a variety of short-time dynamic properties were calculated, except for the rotational self-diffusion coefficient. This missing quantity is included in the present paper. Using a precise hydrodynamic force multipole simulation method, the rotational self-diffusion coefficient is evaluated for concentrated suspensions of permeable particles. Results are presented for particle volume fractions up to 45% and for a wide range of permeability values. From the simulation results and earlier results for the first-order virial coefficient, we find that the rotational self-diffusion coefficient of permeable spheres can be scaled to the corresponding coefficient of impermeable particles of the same size. We also show that a similar scaling applies to the translational self-diffusion coefficient considered earlier. From the scaling relations, accurate analytic approximations for the rotational and translational self-diffusion coefficients in concentrated systems are obtained, useful to the experimental analysis of permeable-particle diffusion. The simulation results for rotational diffusion of permeable particles are used to show that a generalized Stokes-Einstein-Debye relation between rotational self-diffusion coefficient and high-frequency viscosity is not satisfied. © *2011 American Institute of Physics*. [doi:10.1063/1.3604813]

I. INTRODUCTION

The rotational and translational self-diffusion of interacting colloidal and macromolecular particles suspended in a low-molecular-weight solvent is the subject of ongoing research both experimentally and theoretically.[1,2] Originally, self-diffusion in dilute systems was studied; however, the center of interest has shifted since to concentrated dispersions where solvent-mediated many-particle hydrodynamic interactions (HIs) are of central importance. An example, of biological relevance, is self-diffusion of proteins and other macromolecules in the crowded environment of a cell.[3]

Two central quantities quantifying the configuration-averaged influence of HIs on the suspension dynamics are the concentration-dependent short-time rotational and translational self-diffusion coefficients D_r and D_t, respectively. At zero particle concentration, these quantities reduce to the single-particle diffusion coefficients D_0^r and D_0^t. For solvent-impermeable colloidal hard spheres with stick hydrodynamic surface boundary conditions, the single-particle coefficients are given by

$$D_0^{r,\mathrm{hs}} = \frac{k_B T}{8\pi\eta_0 a^3}, \tag{1}$$

$$D_0^{t,\mathrm{hs}} = \frac{k_B T}{6\pi\eta_0 a}, \tag{2}$$

with the Newtonian solvent shear viscosity η_0, the Boltzmann constant k_B, temperature T, and hydrodynamic particle radius a. The influence of the HIs at non-zero concentrations gives rise to values for D_r and D_t smaller than their respective values D_0^r and D_0^t at infinite dilution. The short-time coefficients describe self-diffusion on the time scale $t \ll a^2/D_0^t$, but with t large enough that solvent and particle velocity correlations have decayed. On the colloidal short-time scale, the concentration dependence of D_r and D_t is determined by averaging the HIs with the equilibrium particle distribution.

Self-diffusion coefficients in colloidal suspensions have been determined experimentally by a variety of techniques. The mean-squared displacement (MSD) of partially solvent-index matched suspensions of colloidal spheres[4,5] has been measured as a function of time using dynamic light scattering (DLS), with D_t determined from the initial slope of the MSD.

For the vast majority of systems where this specialized index-matching technique is not applicable, D_t may be inferred, to decent accuracy according to theory and simulation,[6–8] from a first cumulant analysis of the scattered light electric field autocorrelation function, probed at a scattering wavenumber larger than the peak location of the static structure factor where the structure factor attains the value one.[9–11] Translational long-time self-diffusion coefficients not

a)Electronic mail: mekiel@ippt.gov.pl.

considered in the present work can be determined using, e.g., forced Rayleigh scattering,[12,13] fluorescence recovery after photobleaching (FRAP),[2] and fluorescence correlation spectroscopy.[14]

Experimental studies of rotational colloidal self-diffusion are based on techniques which can distinguish different particle orientations. Methods, which have been used for this purpose, are depolarized dynamic light scattering (DDLS) on optically anisotropic particles[15] and nuclear magnetic resonance.[16] More recently developed techniques applicable to a larger variety of systems include time-resolved phosphorescence anisotropy[17,18] and polarized FRAP (Refs. 19 and 20) measurements. The latter methods have been carried out using fluorophore-labeled colloidal particles. Most of the published experimental results deal with self-diffusion properties of monodisperse colloidal systems. However, experimental and theoretical works have been also performed on rotational diffusion in colloidal mixtures, in particular, for binary systems where one component (the tracer) is very dilute.[17,18,20,21] In addition, the DDLS measurements of the rotational diffusion of tracer spheres in a polymeric solution have been used to infer viscoelastic properties from a frequency-dependent generalized Stokes-Einstein-Debye (GSED) relation.[22]

From a simulation method's viewpoint, short-time rotational self-diffusion in monodisperse colloidal systems of non-permeable spheres with excluded volume interactions was studied, e.g., using lattice-Boltzmann (LB),[23] Stokesian dynamics,[24] and accelerated Stokesian dynamics (ASD) simulations.[7] Moreover, virial expansion results of varying accuracy have been derived for the rotational self-diffusion coefficient up to quadratic order in the concentration.[15,25–28]

While there has been no theoretical work so far on rotational self-diffusion in concentrated suspensions of porous particles, other transport properties of porous particles have been studied, including the high-frequency shear viscosity,[29–32] and to first order in concentration the mean sedimentation velocity.[33]

In our earlier work on the short-time dynamics of concentrated suspensions of uniformly porous particles, a broad spectrum of dynamic properties has been calculated, including the hydrodynamic function[8,34] and sedimentation coefficient,[8] translational self-diffusion coefficient,[8,34] and the high-frequency-limiting shear viscosity η_∞.[35,36] These simulation studies were amended by the derivation of easy-to-use approximate analytic expressions of good accuracy, notably a generalized Saito formula for the shear viscosity,[36] and a spherical annulus model approximation for η_∞,[36] and to first order in concentration also for D_t and D_r.[37] Additionally, precise values for the first-order virial coefficients of D_r and D_t corresponding to two-body HIs have been obtained.[37]

In all these studies on permeable particles, the solvent flow inside the spheres is described by the Debye-Büche-Brinkman equation,[38,39] and the particles are assumed to interact directly by excluded volume (i.e., hard-sphere type) forces. Our simplified particle model is specified by two parameters only, namely, the particle volume fraction $\phi = (4\pi/3)na^3$, where n is the number concentration, and the ratio, x, of the particle radius, a, to the hydrodynamic penetration depth, κ^{-1}, inside a permeable sphere. Large (low) values of x correspond to weakly (strongly) permeable particles. Typical values for x in permeable-particle systems, such as core-shell particles, are in the range of $x \sim 30$ or larger.[40] While a specific intra-particle structure is ignored in the model, it is generic in the sense that a more complex internal hydrodynamic structure can be approximately accounted for in terms of a mean permeability. Porous-particle systems of current interest include dendrimers,[41–43] microgel particles ,[44–46] core-shell particles,[40,47–49] and starlike polymers of lower functionality.[50]

The present work complements our earlier analysis of the short-time dynamics in concentrated suspensions of uniformly permeable spheres by giving simulation results and a theoretical analysis of the short-time rotational diffusion coefficient not considered so far at non-dilute concentrations. On employing the multipole simulation method of a very high accuracy[51] encoded in the HYDROMULTIPOLE program package,[28] we calculate the short-time rotational self-diffusion coefficient, $D_r(x, \phi)$, as a function of x and ϕ. Our results cover the full range of porosities, with the volume fraction extending up to 0.45. In combination with recently obtained tabulated values for the first-order virial coefficients of $D_r(x, \phi)$ and $D_t(x, \phi)$,[37] and precise HYDROMULTIPOLE simulation results for $D_t(x, \phi)$ obtained earlier,[8,34] we show that both $D_r(x, \phi)$ and $D_t(x, \phi)$ can be scaled, in the whole range of permeabilities and volume fractions, to the self-diffusion coefficients $D_r^{hs}(\phi) = D_r(\infty, \phi)$ and $D_t^{hs}(\phi) = D_t(\infty, \phi)$ of non-permeable hard spheres with stick boundary conditions and the same size. From these scaling relations, accurate analytic expressions for $D_r(x, \phi)$ and $D_t(x, \phi)$ are obtained. We expect these expressions to be useful in the experimental data analysis of diffusion measurement on permeable particle systems. The present simulation results for $D_r(x, \phi)$ and known results for $\eta_\infty(x, \phi)$ are used to show the violation of a GSED relation between $D_r(x, \phi)$ and $\eta_\infty(x, \phi)$, amending our earlier study of similar GSE relations in Ref. 35.

The paper is organized as follows: Section II provides the theoretical background on short-time self-diffusion of permeable particles. Furthermore, it includes our simulation results for rotational self-diffusion. The scaling relations allowing to map permeable to non-permeable hard-sphere systems are discussed in Sec. III. In Sec. IV, we complete the scaling relations by providing simple expressions for the scaling functions for non-permeable hard spheres. We also discuss the special case of non-permeable hard spheres in comparison to earlier simulations and experimental work. In Sec. V, we demonstrate the violation of the GSED relation. In Sec. VI, we explicitly write convenient expressions for $D_r(x, \phi)$ and $D_t(x, \phi)$ which should prove useful in practical applications. We conclude that with the present paper on self-diffusion in combination with earlier simulation results for other dynamic properties, such as the hydrodynamic function and viscosity, and the development of accurate analytic approximations for these properties,[8,35–37] we have obtained an essentially complete description of the short-time dynamics of uniformly permeable particles with no-overlap interactions.

TABLE I. Simulation results for the normalized short-time rotational self-diffusion coefficient $D_r(x,\phi)/D_0^r(x)$.

$\phi \setminus x$	5	10	20	30	50	100	∞
0.05	0.995	0.987	0.980	0.977	0.973	0.970	0.967
0.15	0.983	0.958	0.934	0.922	0.911	0.901	0.888
0.25	0.968	0.925	0.881	0.860	0.839	0.820	0.796
0.35	0.951	0.886	0.820	0.788	0.757	0.729	0.690
0.45	0.932	0.842	0.753	0.711	0.669	0.629	0.576

II. SHORT-TIME ROTATIONAL SELF-DIFFUSION: THEORY AND RESULTS

Like in our earlier work on the dynamics of permeable particle systems,[8,34–37] we employ a model of uniformly permeable spheres of radius a, dispersed in a Newtonian fluid of viscosity η_0. The low-Reynolds number incompressible flow inside and outside the spheres is described, respectively, by the Stokes[52,53] and Debye-Bueche-Brinkman[38,39] equations,

$$\eta_0 \nabla^2 \boldsymbol{v}(\boldsymbol{r}) - \eta_0 \kappa^2 \chi(\boldsymbol{r})[\boldsymbol{v}(\boldsymbol{r}) - \boldsymbol{u}_i(\boldsymbol{r})] - \nabla p(\boldsymbol{r}) = 0. \quad (3)$$

Here, $\boldsymbol{v}$ and $\boldsymbol{p}$ are the fluid velocity and pressure, respectively, and κ^{-1} is the hydrodynamic penetration depth. The characteristic function, $\chi(\boldsymbol{r})$, is equal to one for the field point $\boldsymbol{r}$ inside any of the spheres and zero outside. The skeleton of a particle i, centered at $\mathbf{r}_i$, moves rigidly with the local velocity $\boldsymbol{u}_i(\mathbf{r}) = \mathbf{U}_i + \boldsymbol{\omega}_i \times (\mathbf{r} - \mathbf{r}_i)$, determined by the translational and rotational velocities $\mathbf{U}_i$ and $\boldsymbol{\omega}_i$, respectively. The fluid velocity and stress change continuously across a particle surface.

The short-time rotational self-diffusion coefficient of a quiescent, isotropic system is given in frame-invariant notation by [21,28]

$$D_r = \frac{k_B T}{3} \left\langle \frac{1}{N} \sum_{i=1}^{N} \mathrm{Tr}\, \boldsymbol{\mu}_{ii}^{rr}(\mathbf{X}) \right\rangle, \quad (4)$$

where $\mathbf{X} = \{\mathbf{r}_1, \cdots, \mathbf{r}_N\}$ is the configuration of $N \gg 1$ sphere centers and Tr denotes the trace operation. The hydrodynamic mobility tensor, $\boldsymbol{\mu}_{ii}^{rr}(\mathbf{X})$, linearly relates the torque acting on a particle i to its rotational velocity, for zero forces and torques exerted on the other particles. For the present model system, the average $\langle \cdots \rangle$ is taken over an equilibrium distribution of non-overlapping spheres, consistent with the periodic boundary conditions used in our simulations. Our numerical calculation of $D_r(x,\phi)$ makes use of Eq. (4).

The coefficient D_r is a function both of x and ϕ. At infinite dilution, Eq. (4) reduces to [54,55]

$$D_0^r(x) = \frac{k_B T}{8\pi \eta_0 a^3 \left[1 + \frac{3}{x^2} - \frac{3 \coth x}{x}\right]}. \quad (5)$$

Note here that $D_0^r(x) > D_0^{r,\mathrm{hs}}$ unless $x = \infty$.

We have calculated $D_r(x,\phi)$ to high precision using a hydrodynamic multipole method corrected for lubrication[28,51,56,59] and encoded in the HYDROMULTIPOLE program package extended to permeable spheres. The hydrodynamic particle structure enters into the HYDROMULTIPOLE method only through a single-particle friction operator, whose form is known for a variety of particle models, such as solid spheres, drops, bubbles, and porous and core-shell particles.[54–57] The single-particle friction operator determines the fluid flow perturbed by the particle immersed in a given ambient flow. For a uniformly permeable particle, the exterior and interior fluid flows can be found by this method with a very high precision, extending in this way the results from Ref. 58 obtained by another method. The details of our simulation method are given elsewhere.[8]

The values for D_r presented in the following have been determined from equilibrium configuration averages over typically $N = 256$ particles in a periodically replicated cubic simulation box, using 100 initial random configurations for each set of parameters. This gives a statistical relative error of less than 0.001. In our multipole expansion method used for the rotational mobility tensor in Eq. (4), the multipole order, L, was truncated usually at $L = 3$. To gain high-precision data, extrapolations to $L \to 8$ were made, leading to an accuracy in D_r better than 1%. The calculated values

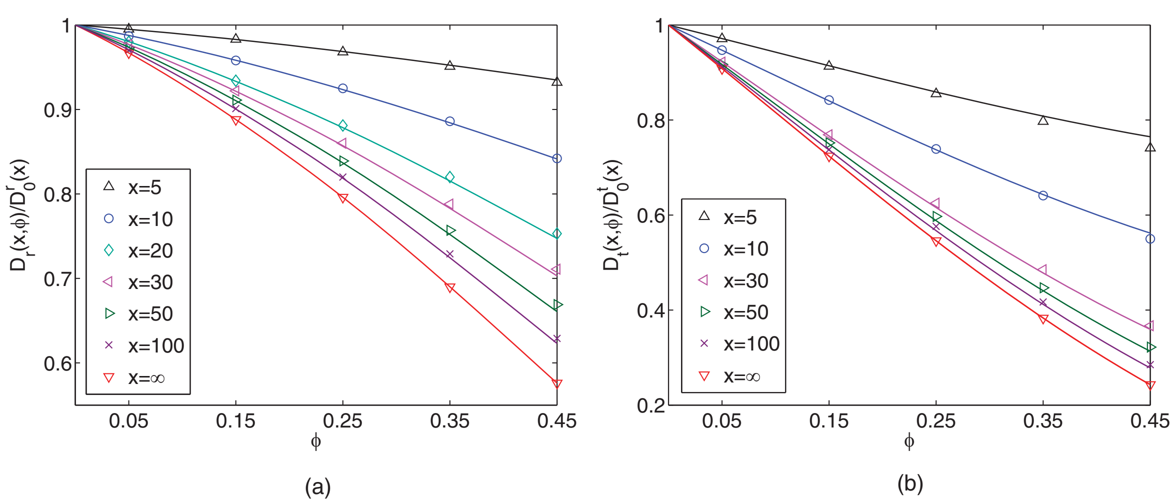

FIG. 1. Rotational (left) and translational (right) self-diffusion coefficients, $D_r(x,\phi)/D_0^r(x)$ and $D_t(x,\phi)/D_0^t(x)$, as functions of ϕ, for values of x as indicated. Symbols: simulation results. Solid lines: interpolated rhs of Eqs. (13) and (14).

for $D_r(N)$ using the periodic simulation box with N particles are not critically dependent on the system size, since $D_r(N=\infty) - D_r(N)$ scales with the particle number such as $1/N$. This system size dependence is similar to that of the high-frequency viscosity, $\eta_\infty(x, \phi)$, of permeable particles. The latter was calculated in earlier work.[29,36]

Table I lists our high-precision simulation results for $D_r(x, \phi)$, for volume fractions up to $\phi = 0.45$. Values of the inverse (reduced) penetration depth x are considered from a very small value $x \sim 5$, characteristic of highly permeable particles, up to $x = \infty$ characteristic of dry particles with stick surface boundary conditions.

III. SCALING SELF-DIFFUSION OF PERMEABLE TO NON-PERMEABLE PARTICLES

From analyzing the numerical data for the rotational self-diffusion coefficient in Table I, we have found an interesting scaling of permeable to non-permeable spheres of the same size. In addition, we found that a similar scaling is valid for the translational self-diffusion coefficient. Therefore, results for both quantities will be given in this section. We start from a brief comparison of $D_r(x, \phi)$ to $D_t(x, \phi)$.

The simulation results for $D_r(x, \phi)$ from Table I are depicted in the left panel of Fig. 1 using symbols. For comparison, the right panel of Fig. 1 shows the corresponding simulation results for $D_t(x, \phi)$ taken from Ref. 8. For permeable particles, the fluid is allowed to penetrate so that the strength of the HIs is decreasing with increasing permeability, i.e., decreasing x. This is the reason for the larger values of D_r and D_t at larger permeabilities. Our results show that the effect of HIs on D_r is weaker than on D_t, i.e., for a given x and ϕ, the reduction of the self-diffusion coefficient relative the infinite dilution value is smaller for rotational diffusion.

The numerical results for $D_r(x, \phi)$ and $D_t(x, \phi)$ plotted in Fig. 1 have significantly different slopes at small volume fractions ϕ. On the other hand, these slopes are well reproduced by the first-order virial coefficients, $\lambda_r(x)$ and $\lambda_t(x)$, defined by the following relations:

TABLE II. First-order virial terms, $\lambda_r(x)$ and $\lambda_t(x)$, of the rotational and translational self-diffusion coefficients (Ref. 37).

x	5	10	20	30	50	100	∞
λ_r	−0.097	−0.236	−0.376	−0.442	−0.505	−0.561	−0.631
λ_t	−0.569	−1.060	−1.416	−1.550	−1.661	−1.746	−1.832

$$\frac{D_r(x,\phi)}{D_0^r(x)} = 1 + \lambda_r(x)\phi + \mathcal{O}(\phi^2) \tag{6}$$

$$\frac{D_t(x,\phi)}{D_0^t(x)} = 1 + \lambda_t(x)\phi + \mathcal{O}(\phi^2)\,, \tag{7}$$

evaluated in Ref. 37 and listed in Table II. The single-particle rotational diffusion coefficient, $D_0^r(x)$, has been already given in Eq. (5), and the translational one has the form given in[38,39]

$$D_0^t(x) = \frac{k_B T}{6\pi\eta_0 a}\left(1 + \frac{1}{x\coth x - 1} + \frac{3}{2x^2}\right). \tag{8}$$

Therefore, the idea is to introduce the following scaling functions:

$$u_r(x,\phi) = \left(\frac{D_r(x,\phi)}{D_0^r(x)} - 1\right)\frac{1}{\lambda_r(x)}\,, \tag{9}$$

$$u_t(x,\phi) = \left(\frac{D_t(x,\phi)}{D_0^t(x)} - 1\right)\frac{1}{\lambda_t(x)}\,. \tag{10}$$

For all values of $x \geq 5$, the functions $u_r(x, \phi)$ and $u_t(x, \phi)$ do practically not depend on x, i.e., they are permeability independent. Indeed, as shown in Fig. 2, the curves for u_r and u_t as functions of ϕ collapse on the corresponding curves for the non-permeable solid spheres, i.e.,

$$u_r(x,\phi) \approx u_r(\infty,\phi)\,, \tag{11}$$

$$u_t(x,\phi) \approx u_r(\infty,\phi)\,, \tag{12}$$

with a relative error less than 3% for $x \geq 10$.

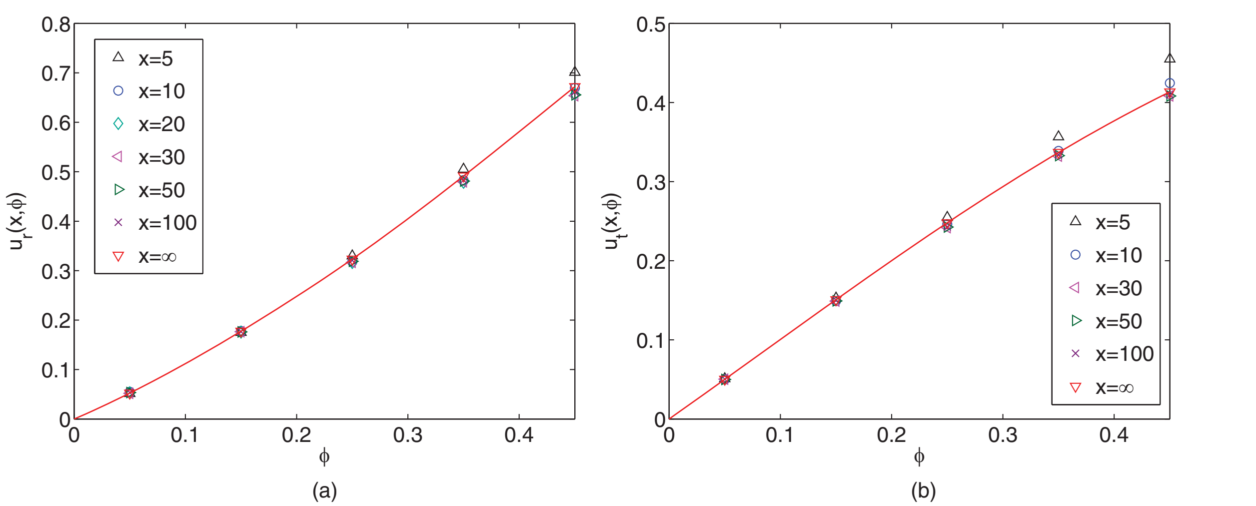

FIG. 2. The functions $u_r(x, \phi)$ and $u_t(x, \phi)$ are practically independent of x. Symbols: simulation results for the indicated values of x. Solid lines: spline fit interpolations of $u_r(\infty, \phi)$ and $u_t(\infty, x)$.

Therefore, the short-time self-diffusion coefficients in suspensions of permeable particles are well approximated by the following expressions:

$$\frac{D_r(x,\phi)}{D_0^r(x)} \approx 1 + \lambda_r(x) u_r(\infty,\phi)\,, \tag{13}$$

$$\frac{D_t(x,\phi)}{D_0^t(x)} \approx 1 + \lambda_t(x) u_t(\infty,\phi)\,. \tag{14}$$

In Fig. 1, the solid, continuous lines are not just mere fits to the simulation data, but represent the expressions in Eqs. (13) and (14), i.e., the outcome of the interesting scaling behavior of the short-time self-diffusion of permeable particles. The error made in using Eqs. (13) and (14) instead of the precise simulation values, is at most 1% for rotational and 3% for translational self-diffusion. To complete the analysis, we need to specify the scaling functions for the non-permeable solid spheres. This will be done in Sec. IV.

IV. SELF-DIFFUSION COEFFICIENTS OF NON-PERMEABLE SPHERES

We will now use the existing data for non-permeable hard spheres to construct simple approximate expressions for the scaling functions $u_r(\infty,\phi)$ and $u_t(\infty,\phi)$.

We start with a comparison between our present simulation results for $D_r^{hs}(\phi) = D_r(\infty,\phi)$ and $D_t^{hs}(\phi) = D_t(\infty,\phi)$ for vanishing permeability, and a selection out of a large body of published experimental (see, e.g., Refs. 4, 6, 15, 16, and 18) and simulation (see, e.g., Refs. 7, 23, 24, 29, 60–62, and 63) data on impermeable hard spheres.

Related to this comparison, we note first that numerical results of varying precision have been published for the first and second virial coefficients of the rotational[15,25–27] and translational[26,27,64] self-diffusion coefficients. High-precision second-order virial expansion results,

$$\frac{D_r^{hs}}{D_0^{r,hs}} = 1 - 0.631\phi - 0.726\phi^2 + \mathcal{O}(\phi^3)\,, \tag{15}$$

$$\frac{D_t^{hs}}{D_0^{t,hs}} = 1 - 1.8315\phi - 0.219\phi^2 + \mathcal{O}(\phi^3)\,, \tag{16}$$

have been obtained by Cichocki *et al.*[28] using the multipole expansion with a lubrication correction for the three-body HIs contributions.

Regarding rotational diffusion, Fig. 3(a) shows the comparison of our data with Lattice-Boltzmann[23] and ASD (Ref. 7) simulation results, and DDLS experimental data[15] for optically anisotropic fluorinated polymer particles. The rotational diffusion coefficient as a function of ϕ has a concave shape, different from that for D_t which is weakly convex. Our simulation data for non-permeable particles agree well with the ASD result. The LB data at large ϕ are somewhat smaller. The key message conveyed by Fig. 3(a) is that the second-order virial result for $D_r^{hs}(\phi)$ in Eq. (15) describes the simulation and experimental data remarkably well for all volume fractions up to the freezing transition value 0.49,[7,23] indicating that higher-order virial coefficients are small or mutually cancel out. Therefore, for constructing a simple approximation for $u_r(\infty,\phi)$ from Eq. (9), it is sufficient to take as $D_r(\infty,x)$ the second-order virial expansion in Eq. (15). In this way, the rotational scaling function is approximated by

$$u_r(\infty,\phi) \approx \phi + 1.151\phi^2\,, \tag{17}$$

with an accuracy of 1.5% or better relative to our simulation data.

In Fig. 3(b), we compare our simulation data for $D_t^{hs}(\phi)/D_0^{t,hs}$ with ASD simulation[7] and force multipole calculation results,[60] and with DLS experimental data.[6] The figure shows that the translational second-order virial expression

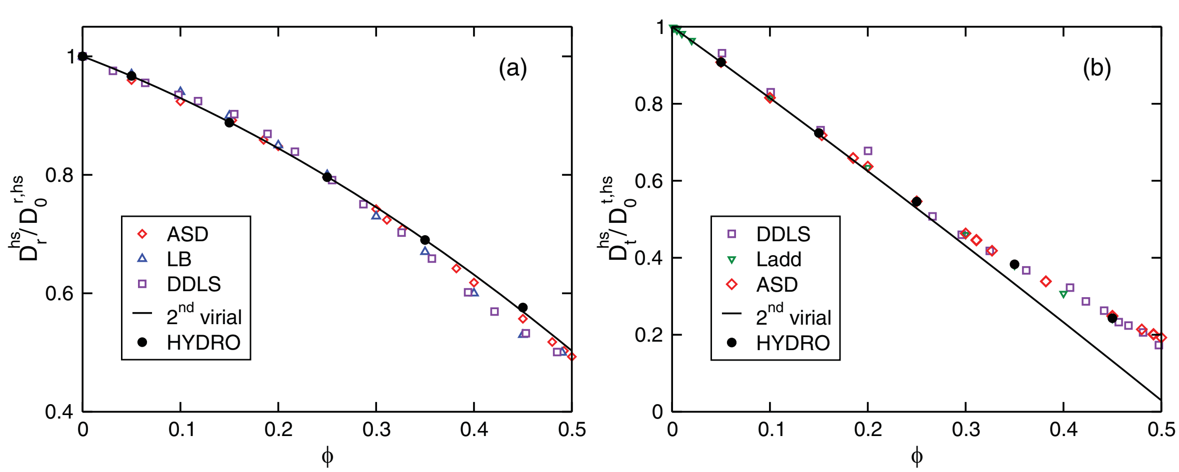

FIG. 3. (a) Rotational and (b) translational self-diffusion coefficients of non-permeable hard spheres with stick boundary conditions, as functions of ϕ. Compared in (a) are our HYDROMULTIPOLE data (labeled HYDRO) for D_r^{hs}/D_0^{hs} with ASD (Ref. 7) and LB (Ref. 23) simulation results, and DDLS experimental data (Ref. 15) for optically anisotropic particles. In (b), we compare the HYDROMULTIPOLE data for $D_t^{hs}(\phi)/D_0^{t,hs}$ with ASD simulation results (Ref. 7), force multipole calculations by Ladd (Ref. 60), and DLS experimental data by Segre *et al.* (Ref. 6). Solid lines: second-order virial expansion results, in (a) according to Eq. (15), and in (b) according to Eq. (16).

in Eq. (16) for D_t^{hs} noticeably underestimates the simulation and experimental data when ϕ is larger than 0.3.

For this reason, we need a more precise expression for $D_t(\infty, \phi)$ than the second-order virial expansion in Eq. (16). We have found that our simulation data are approximated with a 0.4% accuracy by the following expression for the scaling function $u_t(\infty, \phi)$, defined in Eq. (10),

$$u_t(\infty, \phi) \approx \phi + 0.12\phi^2 - 0.65\phi^3 \,. \tag{18}$$

The term $\phi + 0.12\phi^2$ follows from the virial expansion in Eq. (16), and the coefficient of the third-order term, $-0.65\,\phi^3$, has been obtained by fitting to the numerical data for $u_t(\infty, \phi) - \phi - 0.12\phi^2$, in the range $0 \le \phi \le 0.45$.

V. GENERALIZED STOKES-EINSTEIN-DEBYE RELATION

We proceed with the discussion of a generalized short-time GSED relation. Having obtained in this paper precise numerical data for $D_r(x, \phi)$ and taking values of $\eta_\infty(x, \phi)$ tabulated in Ref. 36, we are in position to test the validity of the following short-time GSED relation,

$$\frac{D_r(x, \phi)}{D_0^r(x)} \, \frac{\eta_\infty(x, \phi)}{\eta_0} \overset{?}{\approx} 1 \,, \tag{19}$$

between the rotational self-diffusion coefficient and the high-frequency viscosity of permeable particles. The validity of generalized Stokes-Einstein relations, such as the present one, is an important issue in microrheological studies where one tries to infer rheological properties more easily from diffusion measurements. The GSED relation in Eq. (19) was shown before to be violated for suspensions of non-permeable neutral and charged particles.[18,65] Here, we ask the same validity question for permeable particle systems.

In Fig. 4, the GSED relation is examined for different values of x. If valid, all curves should collapse on a single horizontal line of unit height. One notices from the figure that the GSED relation is significantly violated for $x \ge 30$, and volume fractions $\phi > 0.15$ where the particles are significantly correlated. Thus, a rotating particle experiences its neighborhood not just as a structureless medium characterized by the viscosity $\eta_\infty(x, \phi)$. The GSED relation is, therefore, significantly violated for non-dilute suspensions, unless the permeability is unrealistically large.

The GSED relation for rotational diffusion is more strongly violated than its translational counterpart. As shown in Ref. 35, $(D_t/D_0^t) \times (\eta_\infty/\eta_0)$ increases practically linearly in ϕ, even for non-permeable particles, whereas in Fig. 4, a pronounced nonlinear increase is observed. The GSED test for the rotation of porous particles presented in this paper complements earlier GSE performance tests[35] of different short-time diffusion properties. Of all considered GSE relations, only the one for the cage diffusion coefficient can claim a certain validity when applied to neutral porous particles.[35] However, also this relation becomes invalid when the particles are significantly charged.[7]

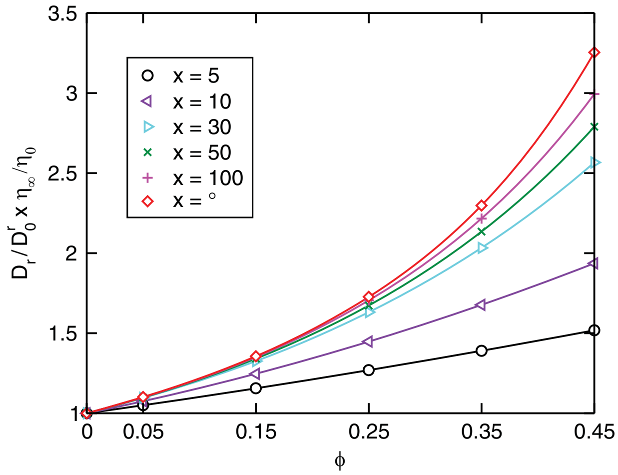

FIG. 4. The generalized Stokes-Einstein-Debye relation between $D_r(x, \phi)$ and high-frequency viscosity $\eta_\infty(x, \phi)$ is not satisfied. Solid lines are interpolating spline fits to our simulation results (symbols).

VI. CONCLUSIONS

Using the HYDROMULTIPOLE simulation method, the short-time rotational self-diffusion coefficient, $D_r(x, \phi)$, of uniformly permeable spheres was calculated to high precision as a function of permeability and volume fraction.

An interesting scaling relation was found between $D_r(x, \phi)$ and the corresponding coefficient, $D_r(\infty, \phi)$, of non-permeable, solid spheres of the same size, where the permeability enters only through the first-order rotational virial coefficient. A similar scaling was found for translational self-diffusion.

The combination of the scaling relations with accurate second-order and third-order concentration expansion results in Eqs. (17)–(18) for $D_r(\infty, \phi)$ and $D_t(\infty, \phi)$, respectively, has led us to the expressions,

$$\frac{D_r(x, \phi)}{D_0^r(x)} \approx 1 + \lambda_r(x)\phi\,(1 + 1.151\,\phi)\,, \tag{20}$$

$$\frac{D_t(x, \phi)}{D_0^t(x)} \approx 1 + \lambda_t(x)\phi(1 + 0.12\,\phi - 0.65\,\phi^2)\,, \tag{21}$$

for the permeability-dependent self-diffusion coefficients. In combination with Table II for λ_r and λ_t, these are convenient expressions useful in diffusion measurement analysis of permeable particle systems. The accuracy of these expressions is better than 1.5% for rotational and 3.5% for translational self-diffusion, for the whole range of volume fractions $\phi \le 0.45$ provided $x \ge 5$.

We expect the expressions to be useful in the experimental analysis of self-diffusion, to gain a quick estimate of the mean porosity in concentrated systems. Moreover, they can serve as short-time inputs into theoretical methods of calculating frequency-dependent and long-time diffusion properties, such as in mode-coupling and dynamic density functional theory methods. We also used the simulation results for $D_r(x, \phi)$, and our recent results for $\eta_\infty(x, \phi)$ to show that the generalized Stokes-Einstein-Debye relation is significantly violated for non-dilute suspensions, unless the permeability is unrealistically large.

Dispersions of spherical particles with more complex internal hydrodynamic structure, such as core-shell particles, and different direct interactions, will be the subject of a future study.

ACKNOWLEDGMENTS

M.L.E-J. and E.W. were supported in part by the Polish Ministry of Science and Higher Education Grant No. N501 156538. G.N. thanks M. Heinen for helpful discussions and the Deutsche Forschungsgemeinschaft (SFB-TR6, project B2) for financial support. Numerical simulations were done at NACAD-COPPE/UFRJ in Rio de Janeiro, Brazil, and at the Academic Computer Center in Gdansk, Poland.

[1] P. N. Pusey, in *Liquids, Freezing, and the Glass Transition*, edited by J. P. Hansen, D. Levesque, and J. Zinn-Justin (Elsevier, Amsterdam, 1991).
[2] G. Nägele, J. K. G. Dhont, and G. Meier, in *Diffusion in Condensed Matter*, edited by P. Heitjans and J. Kärger (Springer, Berlin, 2005).
[3] T. Ando and J. Skolnick, Proc. Natl. Acad. Sci. U.S.A. **107**, 18457 (2010); see www.pnas.org/cgi/doi/10.1073/pnas.1011354107.
[4] W. van Megen, S. M. Underwood, and I. Snook, J. Chem. Phys. **85**, 4065 (1999).
[5] A. Brand, H. Versmold, and W. van Megen, J. Chem. Phys. **110**, 1283 (1999).
[6] P. N. Segrè, O. P. Behrend, and P. N. Pusey, Phys. Rev. E **52**, 5070 (1995).
[7] A. J. Banchio and G. Nägele, J. Chem. Phys. **128**, 104903 (2008).
[8] G. C. Abade, B. Cichocki, M. L. Ekiel-Jeżewska, G. Nägele, and E. Wajnryb, J. Chem. Phys. **132**, 014503 (2010).
[9] P. N. Pusey, J. Phys. A **11**, 119 (1978).
[10] P. Holmqvist and G. Nägele, Phys. Rev. Lett. **104**, 058301 (2010).
[11] M. Heinen, P. Holmqvist, A. J. Banchio, and G. Nägele, J. Appl. Crystallogr. **43**, 970 (2010).
[12] W. D. Dozier and P. M. Chaikin, J. Phys. (Paris) **46-C.3**, 165 (1985).
[13] R. Simon, T. Palberg, and P. Leiderer, J. Chem. Phys. **99**, 3030 (1993).
[14] A. Wilk, J. Gapinski, A. Patkowski, and R. Pecora, J. Chem. Phys. **121**, 10794 (2004).
[15] V. Degiorgio, R. Piazza, and R. B. Jones, Phys. Rev. E **52**, 2707 (1995).
[16] J. Kannetakis, A. Tölle, and H. Sillescu, Phys. Rev. E **55**, 3006 (1997).
[17] G. H. Koenderink, H. Zhang, M. P. Lettinga, G. Nägele, and A. P. Philipse, Phys. Rev. E **64**, 2001 (2001).
[18] G. H. Koenderink, H. Zhang, D. G. A. L. Aarts, M. P. Lettinga, A. P. Philipse, and G. Nägele, Faraday Discuss. **123**, 335 (2003).
[19] M. P. Lettinga, G. H. Koenderink, B. W.M. Kuipers, E. Bessels, and A. P. Philipse, J. Chem. Phys. **120**, 4517 (2003).
[20] G. H. Koenderink, "Rotational and translational diffusion in colloidal mixtures," Ph.D. dissertation, Utrecht University, The Netherlands, 2003.
[21] H. Zhang and G. Nägele, J. Chem. Phys. **117**, 5908 (2002).
[22] E. Andablo-Reyes, P. Diaz-Leyva, and J. L. Arauz-Lara, Phys. Rev. Lett. **94**, 106001 (2005).
[23] M. H. J. Hagen, D. Frenkel, and C. P. Lowe, Physica A **272**, 376 (1999).
[24] R. J. Phillips, J. F. Brady, and G. Bossis, Phys. Fluids **31**, 3462 (1988).
[25] C. Urdaneta, D. M. Jones, and M. Muthukumar, J. Chem. Phys. **91**, 5127 (1989).
[26] H. J. H. Clercx and P. P. J. M. Schram, Physica A **174**, 293 (1991).
[27] H. J. H. Clercx and P. P. J. M. Schram, J. Chem. Phys. **96**, 3137 (1992).
[28] B. Cichocki, M. L. Ekiel-Jeżewska, and E. Wajnryb, J. Chem. Phys. **111**, 3265 (1999).
[29] G. Mo and A. S. Sangani, Phys. Fluids **6**, 1637 (1994).
[30] A. A. Potanin and W. B. Russel, Phys. Rev. E **52**, 730 (1995).
[31] S. L. Elliot and W. B. Russel, J. Rheol. **42**, 361 (1998).
[32] P. A. Nommensen, M. H.G. Duits, D. van den Ende, and J. Mellema, Phys. Rev. E **59**, 3147 (1999).
[33] S. B. Chen and A. Cai, J. Colloid Interface Sci. **217**, 328 (1999).
[34] G. C. Abade, B. Cichocki, M. L. Ekiel-Jeżewska, G. Nägele, and E. Wajnryb, Phys. Rev. E. **81**, 020404(R) (2010).
[35] G. C. Abade, B. Cichocki, M. L. Ekiel-Jeżewska, G. Nägele, and E. Wajnryb, J. Phys.: Condens. Matter **22**, 322101 (2010).
[36] G. C. Abade, B. Cichocki, M. L. Ekiel-Jeżewska, G. Nägele, and E. Wajnryb, J. Chem. Phys. **133**, 084906 (2010).
[37] B. Cichocki, M. L. Ekiel-Jeżewska, G. Nägele, and E. Wajnryb, Phys. Fluids (submitted).
[38] H. C. Brinkman, Proc. R. Dutch Acad. Sci. **50**, 618 (1947).
[39] P. Debye and A. M. Bueche, J. Chem. Phys. **16**, 573 (1948).
[40] M. H.G. Duits, P. A. Nommensen, D. van den Ende, and J. Mellema, Colloids Surf. A **183–185**, 335 (2001).
[41] C. N. Likos, S. Rosenfeldt, N. Dingenouts, M. Ballauff, P. Lindner, N. Werner, and F. Vögtle, J. Chem. Phys. **117**, 1869 (2002).
[42] S. Huißmann, A. Wynveen, C. N. Likos, and R. Blaak, J. Phys.: Condens. Matter **22**, 232101 (2010).
[43] Z. Adamczyk, B. Jachimska, and M. Kolasinska, J. Colloid Interface Sci. **273**, 668 (2004).
[44] S. Pyett and W. Richtering, J. Chem. Phys. **122**, 034709 (2005).
[45] T. Eckert and W. Richtering, J. Chem. Phys. **129**, 124902 (2008).
[46] C. A. Coutinho, R. K. Harrinauth, and V. K. Gupta, Colloids Surf. A **318**, 111 (2008).
[47] G. Petekidis, J. Gapiński, P. Seymour, J. S. van Duijneveldt, D. Vlassopoulos, and G. Fytas, Phys. Rev. E **69**, 042401 (2004).
[48] M. Zackrisson, A. Stradner, P. Schurtenberger, and J. Bergenholtz, Langmuir **21**, 10835 (2005).
[49] J. Masliyah, G. Neale, K. Malysa, and T. G.M. van de Ven, Chem. Eng. Sci. **42**, 245 (1987).
[50] C. N. Likos, H. Löwen, M. Watzlawek, B. Abbas, O. Jucknischke, J. Allgaier, and D. Richter, Phys. Rev. Lett. **80**, 4450 (1998).
[51] B. Cichocki, B. U. Felderhof, K. Hinsen, E. Wajnryb, and J. Bławzdziewicz, J. Chem. Phys. **100**, 3780 (1994).
[52] J. Happel and H. Brenner, *Low Reynolds Number Hydrodynamics* (Martinus Nijhoff, Dordrecht, 1986).
[53] S. Kim and S. J. Karrila, *Microhydrodynamics: Principles and Selected Applications* (Butterworth-Heinemann, London, 1991).
[54] B. U. Felderhof and J. M. Deutch, J. Chem. Phys. **62**, 2391 (1975).
[55] R. Reuland, B. U. Felderhof, and R. B. Jones, Physica A **93**, 465 (1978).
[56] B. Cichocki, B. U. Felderhof, and R. Schmitz, PCH, PhysicoChem. Hydrodyn. **10**, 383 (1988).
[57] B. Cichocki and B. U. Felderhof, J. Chem. Phys. **130**, 164712 (2009).
[58] P. Adler, J. Colloid Interface Sci. **81**, 531 (1981).
[59] B. Cichocki, R. B. Jones, R. Kutteh, and E. Wajnryb, J. Chem. Phys. **112**, 2548 (2000).
[60] A. J. C. Ladd, J. Chem. Phys. **93**, 3484 (1990).
[61] A. Sierou and J. F. Brady, J. Fluid Mech. **448**, 115 (2001).
[62] A. J. Banchio and J. F. Brady, J. Chem. Phys. **118**, 10323 (2003).
[63] J. F. Brady, Curr. Opin. Colloid Interface Sci. **1**, 472 (1996).
[64] D. M. Jones, M. Muthukumar, and S. M. Cohen, J. Chem. Phys. **90**, 7542 (1989).
[65] A. J. Banchio, G. Nägele, and J. Bergenholtz, J. Chem. Phys. **111**, 8721 (1999).